

On the Choice of Tool Material in Friction Stir Welding of Titanium Alloys

Gianluca Buffa, Livan Fratini and Fabrizio Micari

Dept. of Dept. of Chemical, Management, Computer Science and Mechanical Engineering
University of Palermo
Palermo, Italy

Luca Settineri

Department of Production Systems and Business Economics
Polytechnic University of Turin

ABSTRACT

Friction Stir Welding (FSW) is a solid state welding process patented in 1991 by TWI; initially adopted to weld aluminum alloys, is now being successfully used also for magnesium alloys, copper and steels. The wide diffusion the process is having is due to the possibility to weld both materials traditionally considered difficult to be welded or “unweldable” by traditional fusion welding processes due to peculiar thermal and chemical material properties, and complex geometries as sandwich structures and straightening panels. Recently, research is focusing on titanium alloys thanks to the high interest that such materials are getting from the industry due to the extremely high strength-weight ratio together with good corrosion resistance properties. At the moment, the main limit to the industrial applicability of FSW to titanium alloys is the tool life, as ultra wear and deformation resistant materials must be used. In this paper a, experimental study of the tool life in FSW of titanium alloys sheets at the varying of the main process parameters is performed. Numerical simulation provided important information for the fixture design and analysis of results. Tungsten and Rhenium alloy W25Re tools are found to be the most reliable among the ones considered.

KEYWORDS

Friction Stir Welding, Titanium Alloys, Tungsten alloys, tool life.

INTRODUCTION

During the last decade, the use of alloys characterized by large resistance-weight ratios has been selected as the best technical solution for automotive as well as aerospace and aeronautical industries. However, besides the several advantages they provide - as increase in the active and passive safety, reduction of fuel consumption and environmental impact - these materials present a few drawbacks that must be properly taken into account. In particular, they are often characterized by lower ductility with respect to steels, anisotropy and are considered difficult to be welded or “non weldable”.

At the moment, traditional fusion welding processes for materials as aluminum, magnesium and titanium alloys is often characterized by the insurgence of defects like porosities and inclusions [1], [2]. In particular, as far as titanium alloys are regarded, further issues are the elevated distortion in the welded joints due to the high temperatures reached and the phase change. Among the alternative

processes proposed, Friction Stir Welding (FSW) appears as one of the most promising continuous joining techniques. FSW is a solid state weld process invented in 1991 in which the effectiveness of the obtained joint is strongly affected by several geometrical and technological parameters; in particular both rotating speed and feed rate have to be properly chosen in order to obtain effective joints [3], [4]. During the process, the tool rotation speed (R) and feed rate (V_f) are combined in a way that an asymmetric metal flow is obtained. In particular, an advancing side and a retreating side are observed: the former being characterized by the “positive” combination of the tool feed rate and of the peripheral tool velocity while the latter having velocity vectors of feed and rotation opposite to each other. Hence the tool action is the main responsible for both the material softening and the material flow resulting in the weld of the two workpieces. Based on the above description, it is clear how the tool plays a key role in the process. In particular, it must possess good mechanical properties at the temperatures reached during the process, being thus

characterized by significantly larger melting temperature and ultimate tensile strength with respect to the material to be welded.

Nowadays, the process can be considered mature for light materials as aluminum and magnesium alloys and it is already being utilized for automotive, aeronautical, civil and naval industrial applications for different joint morphologies [5], [6], [7]. However, as far as titanium alloys are regarded, difficulties arise for the application of the process because of the chemical, mechanical and thermal peculiar properties of these materials. Due to the low thermal conductivity [7 W/mK], resulting in a non uniform temperature distribution and in a significant thermal gradient along the joint thickness, the effectiveness of the joint can be compromised as most of the heat is generated on the top surface of the joint, i.e. the contact surface between the tool shoulder and the sheets. For such reasons a specifically designed clamping fixture must be designed. Additionally, the high reactivity of titanium with atmospheric gas – hydrogen, oxygen and nitrogen – requires a shield inert gas protection for the weld in order to avoid the formation of very hard oxides on the top surface of the sheets to be welded right where the tool is deforming and welding the material.

Finally, due to the high temperatures and contact forces between the sheets and the tool, the choice is limited to ultra resistant, high melting and high cost tool materials. In [8] friction stir welding of L80 steel was investigated with experiments and modeling. Severe tool deformation and some wear were observed when commercially pure tungsten was used. Finite element analysis (FEA) was used to predict the mushrooming of the tool. The temperature histories in the weld region and tool forces were measured and supplied to a finite element model. The simulated pin deformation matched the experimental observation. Using this model and optimization techniques, the required yield strength of the pin material is estimated to be 400 MPa at 1000°C to avoid mushrooming. At the moment, in spite of the recent research efforts, this issue appears as the most severe limitation to the industrial applicability of FSW to titanium alloys as significant deformation can be found on the tool itself even after only a few millimeters of weld length.

In the recent years to two main categories of materials have been utilized: ceramic and refractory metal alloys. Among the former the most commonly utilized are Polycrystalline cubic Boron Nitride (PcBN); although good results have been reached, for a wide industrial utilization of such materials the main limitations consist in the extremely elevated costs as well as in the significant brittleness that may lead to unexpected failures [9]. In [10] friction stir welding was applied to commercial purity titanium using a polycrystalline cubic boron nitride tool, and microstructure and hardness in the weld were examined. Additionally, the microstructural evolution during friction stir welding was also discussed. The stir

zone consisted of fine equiaxed α grains surrounded by serrate grain boundaries, which were produced through the $\beta \rightarrow \alpha$ allotropic transformation during the cooling cycle of friction stir welding. The fine α grains caused higher hardness than that in the base material. A lath-shaped α grain structure containing Ti borides and tool debris was observed in the surface region of the stir zone, whose hardness was the highest in the weld. In [11] it is stated that for ferrous alloys, FSW tool material development is at the heart of the advancement of this novel joining technique. Polycrystalline cubic boron nitride (PCBN) materials, produced via high pressure and high temperature (HPHT) process, have demonstrated good performance in FSW applications. Thus, it is becoming more practical to friction stir weld high melting temperature materials such as stainless steels and alloy steels. The performance of FSW materials is highly dependent on the design of material system. This manuscript presents findings on correlations between material properties and material design such as the choice of binder phases and matrix and their subsequent interactions with ultra-hard particles.

Among the refractory metal alloys researchers focused their attention on Co based and, above all, W based alloys. In this way a significant cost saving can be achieved, opening the doors to a full industrial application of the process. Unfortunately higher wear and deformation are observed for these materials; hence a detailed investigation on their performance during the welding process is needed. In [12] the authors developed a new friction stir welding (FSW) tool that enables welding of high-softening-temperature materials, such as steels, and titanium alloys. The new tool is made of a Co-based alloy strengthened by precipitating intermetallics, $\text{Co}_3(\text{Al,W})$, with an L12 structure at high temperatures. The Co-based alloy tool can be manufactured at a low cost through a simple production method consisting of casting, heat-treatment, and then machining. It exhibits yield strengths higher than 500 MPa at 1000°C, so that it might have great potential as a FSW tool for hard materials. In this study, the feasibility to use the Co-based alloy tool to friction stir weld various high-softening-temperature materials was examined through the analysis of the changes in tool shape during the process and the weld appearances produced. It should be observed that there is a great emphasis on the development of friction stir welding (FSW) tools that are resistant to wear while joining high-temperature materials such as iron, titanium and nickel-based alloys. Wear mechanisms may include deformation, abrasive, and/or adhesive phenomena. In [13] and [14] three different W based materials, were tested performing, with the same tool geometry, FSW tests in the worst, i.e. coldest, conditions on very thick high strength steel (HSS) plates. The probability of adhesive wear between tool and substrate material was evaluated using computational thermodynamics and kinetics models. Adhesive wear was described as diffusion couple between tool and substrate materials. First, the combination of

tungsten tool and titanium base metal was evaluated. The experimental data and calculations showed rapid rate of cross-diffusion at FSW temperatures. Secondly, the combination of tungsten tool and steel was evaluated. The calculations showed minimal degradation due to cross-diffusion. However, microstructural characterization showed alloying of steel with tungsten. Finally the deformation of the welding tools was evaluated finding minimum tool degradation for W25Re and W-Re-hafnium carbon (HfC) tools.

In the paper a quantitative analysis of the tool life in FSW of 3 mm thick Ti-6V-4Al titanium alloy sheets is presented. Three different W based materials have been selected, and each of them was tested under three different process conditions till the complete failure of the tool occurred. An already developed numerical model of the process was utilized both to set up the welding fixture and to provide explanations for the obtained results.

EXPERIMENTS

Ti-6Al-4V titanium alloy sheets 100 mm x 200 mm and 3 mm thick were welded together under different process conditions. In particular rotating speeds of 300, 700 and 1000 rpm were selected, based on a previously developed campaign [15]. Fixed advancing speed equal to 35 mm/min, nuting angle equal to 2° and tool shoulder sinking of 0.2 mm were considered for all the welds. The tool sinking speed was kept constant and equal to 0.6 mm/min for all the welds. It is worthy notice that this parameter is crucial for the tool life, being the sinking stage the most dangerous for the tool as it is in contact with the still cold titanium of the sheets. In this way three different process conditions, characterized by an increasing Specific Thermal Contribution (STC) given to the weld, were taken into account.

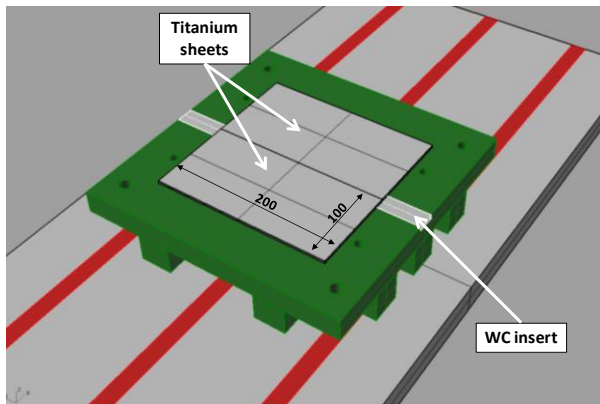


Figure 1. Sketch of the utilized clamping fixture.

A tungsten insert was placed in the backplate along the welding line in order to avoid carbon contamination with the titanium sheets. In Figure 1 a sketch of the utilized fixture is shown.

The tool geometry was the same for each tests at the varying of both tool material and welding conditions ad was characterized by a 16 mm shoulder and a 30° conical pin, 2.6 mm in height and 5 mm in major diameter. The pin had a smooth lateral surface. Due to the relatively small sheet thickness and consequent height of the pin the presence of threads would have resulted in an increased complexity of the tool manufacturing cycle, with limited enhancement of the vertical component of the material flow an of the joint quality. It should be noticed that the maximization of the mechanical properties of the joints is not within the aims of the present work.

Three different materials were utilized: K10, K10-K30 and W25Re. The firsts are two WC based materials, with a certain percentage of cobalt, characterized by an ultrafine grain microstructure. In general, smaller tungsten carbide grain sizes allow for the manufacture of carbides with a finer microstructure. A prerequisite for this is the prevention of grain growth during the sintering process by adding suitable doping components in the right amount, adjusted to the cobalt content. The latter has been determined based on the required performance specifications for the carbide. Since the specific surface of carbide depends reciprocally on its grain size, finely-grained carbide can absorb more binder than a coarsely-grained TC. When considering the ISO hardness curve of carbide in a diagram as a function of the carbide grain size and its cobalt content, the curve behaves as a decreasing polynomial function. An increase in cobalt content results in increased toughness while hardness and wear resistance are reduced. This opposite development of the two desirable parameters, hardness and toughness, can be countered by reducing the carbide grain size. The result is an increased hardness on account of the finer basic grain of the carbide which at the same time permits a high binding metal content as the grain structure offers a large specific surface, allowing for a high toughness. Consequently, superfine grain carbide grades offer increased hardness while almost maintaining toughness. In the next Table 1 the composition, as weight percentage, and the main mechanical properties of these two alloys, as given by the supplier, are reported.

Table 1. chemical composition (wt%) and mechanical properties of the two WC based alloys utilized.

| Material | WC % | Co % | Density [g/cm ³] | Hardness HV10 | Transverse rupture strength (TRS) [MPa] |
|----------|------|------|------------------------------|---------------|---|
| K10 | 95.8 | 4.2 | 15.05 | 2300 | 3700 |
| K10-K30 | 88.0 | 12.0 | 14.10 | 1760 | 4600 |

As far as the W25Re is regarded, the presence of 25% of pure rhenium results in increased recrystallization temperature, ductility and ultimate tensile strength with respect to commercially pure tungsten, due to both solid

solution strengthening and grain size refinement [14]. In Table 2 the mechanical properties - as provided by the supplier - at both room and high temperatures are shown.

Table 2. chemical composition (wt%) and mechanical properties of W25Re

| Material | W % | Re % | Density [g/cm ³] | E [Gpa] | Tensile strength (20°C) [MPa] | Tensile strength (1500°C) [MPa] |
|----------|------|------|------------------------------|---------|-------------------------------|---------------------------------|
| W25Re | 75.0 | 25 | 19.7 | 410 | 3800 | 330 |

As far as the utilized experimental procedure is regarded, once selected the tool material, cooling conditions and process parameters, i.e. tool rotating speed, several welds, each about 180 mm in length, were performed till the failure of the tool. In this way tool life diagrams were built as will be shown in the next paragraphs. Figure 2 shows the final part of a weld characterized by 700 rpm; the thermal flow conferred to the weld is visible even at naked eye: the dotted line traces the boundaries of the Heat Affected Zone (HAZ) which, in spite of the extremely poor thermal conductivity of titanium, is quite large.

the rotating tool and two different configurations were tested: in the first water is inserted in the cage, cooling the top portion of the tool, i.e. the one farer from the pin, while a shielding argon flow was given to the sheets in the welding area. In the second configuration no water was considered and the argon was introduced directly in the cage in order to have a circumferential gas flow. Figure 3 (a and b) shows a sketch of these configurations.

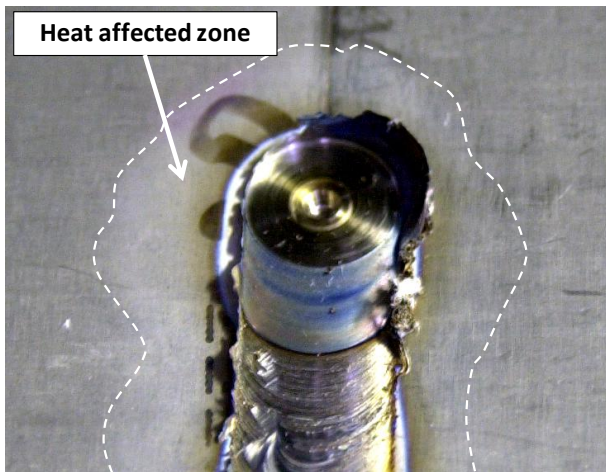
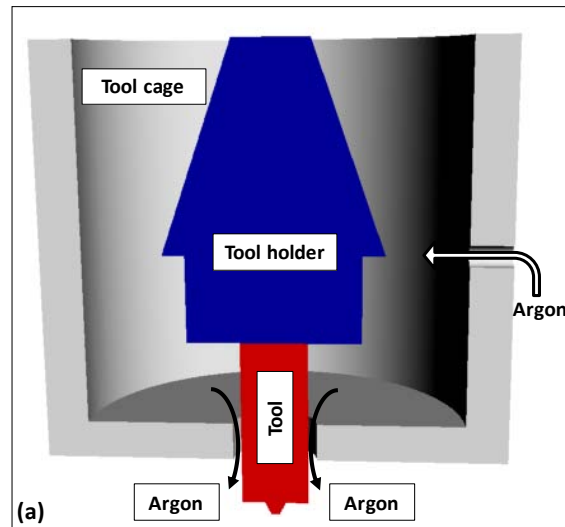


Figure 2. Final portion of the weld obtained with R = 700 rpm; different material color on the top surface indicates the Heat Affected Zone.

In order to investigate the possibility to enhance the tool life, the effect of water cooling of the tool was considered. In particular a fixed cylindrical “cage” was placed around



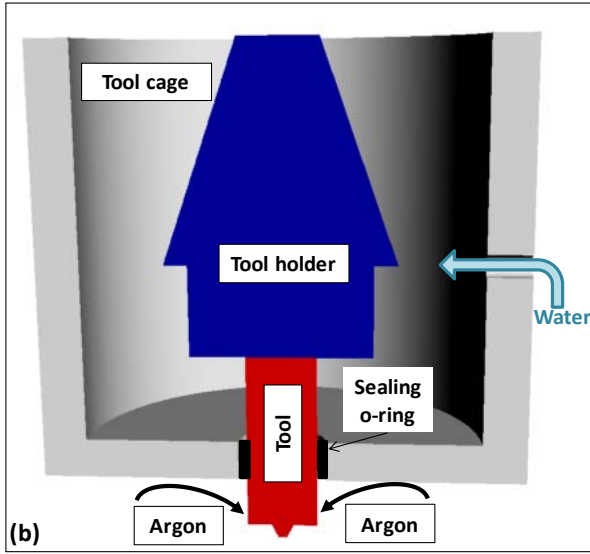


Figure 3. Sketches of the no water (a) and water (b) tool cooling configurations.

NUMERICAL MODEL

The commercial FEA software DEFORM-3D™, Lagrangian implicit code designed for metal forming processes, was utilized to investigate the FSW of Titanium alloys. The numerical simulation was divided into two stages: the sinking stage and the welding (advancing) one. During the sinking stage, simulated to reach high enough temperature level for the subsequent welding process, the tool moves down vertically at 0.6 mm/sec with the assigned rotating speed. Then, during welding or advancing stage, the rotating tool moves along the welding line (seam). As far as the thermal characteristics of the considered Ti-6Al-4V alloy are regarded, constant values, taken from literature [16], [17] were selected. In particular thermal conductivity equal to 14 [N/s°K] and heat capacity equal to 3.4 [N/mm²°K] were utilized. This assumption makes the thermal problem linear speeding up the numerical solution at each time increment.

A temperature, strain and strain rate dependent rigid-viscoplastic flow stress was used to model the plastic behavior. Further details on the model and the material data can be found in [18] and [19]. The tool and the components of the clamping fixture, namely the backplate and the WC insert, were modeled as rigid bodies and meshed, for the thermal analysis, with about 5,000 and 15,000 and 8,000 tetrahedral elements, respectively. The upper part of the clamping fixture (i.e. the actual clamping system) was modeled through proper boundary conditions given to the work-piece. A “single block” continuum model is used to model the workpiece in order to avoid contact instabilities due to the intermittent contact at the sheet-sheet interfaces. The sheet blanks were meshed with about 20,000 tetrahedral elements with single edges of about 0.75mm; in

this way about four elements were placed along the sheet thickness. A non-uniform mesh with adaptive re-meshing was adopted with smaller elements close to the tool and a re-meshing referring volume was identified all along the tool feed movement [20]. In Figure 4 a close up of the single block sheet at the end of the sinking stage is shown.

The contact conditions at the tool-workpiece interface were modeled through a constant interface heat exchange coefficient of 11[N mm⁻¹ s⁻¹ °C⁻¹] and a constant shear friction factor equal to 0.3. The latter was chosen in such a way to maximize the fitting of the numerical results with experiments. Details on the contact modeling can be found in [18] and [20].

As far as the modeling of the two different tool cooling conditions is regarded, the “no water” case study was modeled prescribing, for the whole lateral surface of the tool, a convective heat exchange with forced gas (see again Figure 2a) characterized by a coefficient of 2 [N mm⁻¹ s⁻¹ °C⁻¹]. On the other hand, the water cooled case study was modeled by dividing the tool lateral surface into three areas: in the top area thermal exchange with water was considered through a convection coefficient equal to 15 [N mm⁻¹ s⁻¹ °C⁻¹]; for the central area no heat exchange with environment was assigned, being in direct contact with the sealing o-ring needed in order to avoid water leaking on the sheets to be welded (see again Figure 2b); finally, forced air convection was modeled in the bottom area of the tool by a thermal exchange coefficient equal to 2 [N mm⁻¹ s⁻¹ °C⁻¹] [17]. In the following Figure 5 (a and b) the model of the tool is presented and a sketch of the different areas considered for thermal exchange phenomena is shown.

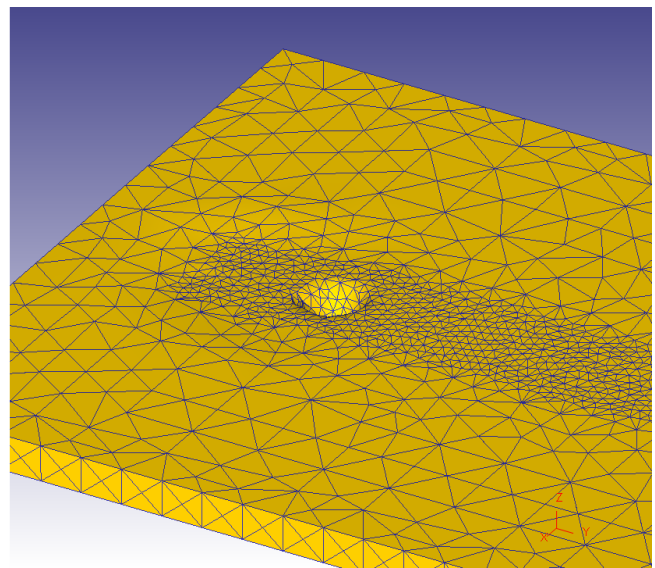


Figure 4. Sketch of the continuum sheet model at the beginning of the welding stage.

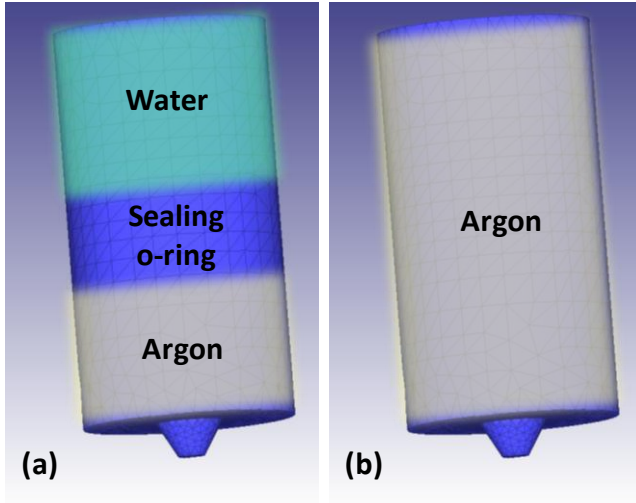


Figure 5. Tool model and sketch of the different areas considered for thermal exchange phenomena modeling: water cooling (a) and no water (b) case studies.

RESULTS

The effectiveness of the tool water cooling was assessed at the beginning of the experimental campaign with the aid of the numerical tool. Two simulations, characterized by tool rotational speed of 700 rpm, were run at the varying of the thermal exchange conditions as described in the previous paragraph. Figure 6 shows the obtained temperature profiles in a longitudinal section of the tool taken once the process reached the steady state, that is after the tool advanced for about 22 mm.

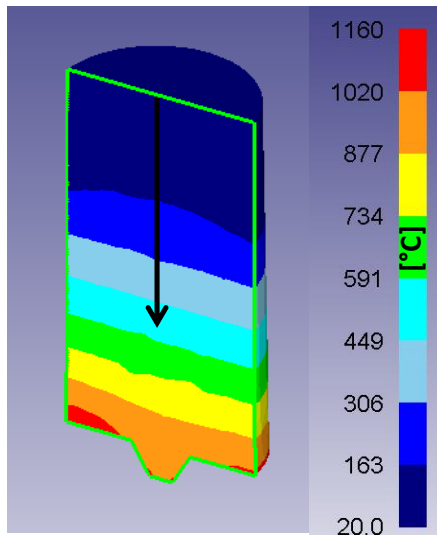


Figure 6. Temperature profiles in a tool longitudinal section after the process reached the steady state (tool rotation 700 rpm, no water case study).

As it can be observed from the above figure, although the maximum temperature reached is quite high, the top area of the tool remains “cold” due to the very poor thermal conductivity of the WC based alloys. Based on this observation it was deduced that the possible use of a coolant chiller would not result in a significant reduction on the tool temperature. In order to perform a quantitative comparison between the two case studies, the temperatures along the tool axis (see the black arrow in Figure 6) have been collected for both the water and the no water case study. In the next Figure 7 the obtained curves are shown. As it could be expected after the analysis of Figure 6, no significant difference can be observed all along the tool length; just close to the top of the tool a slightly lower temperature is calculated for the water case study. Based on these preliminary results, just one set of experiments was performed at the varying of the tool cooling conditions. In particular the K10-K30 tool and rotating speed of 700 rpm were utilized. Almost identical results were obtained in terms of tool life, as suggested by the results obtained with the numerical model, and hence, for the following experiments, just the no water configuration was taken into account.

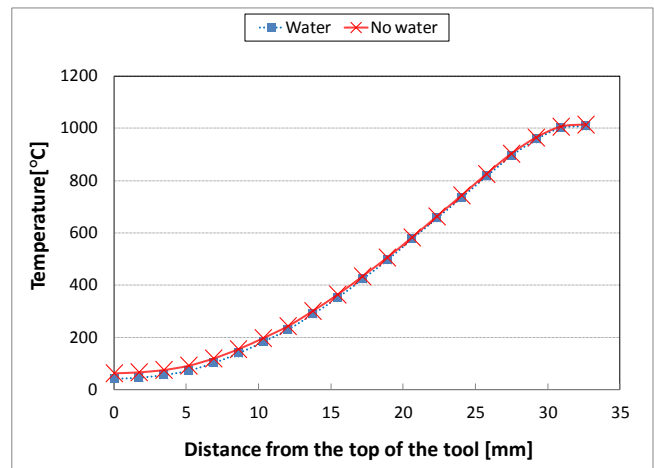


Figure 7. Temperature profiles in a tool longitudinal section for the water and no water case studies.

As briefly mentioned in the introduction paragraph, the experimental strategy was to select a tool material and a process condition, i.e. a tool rotating speed value, being constant all the other process parameters. Then, several sheets were welded together, with the given configuration, till the complete failure of the tool. In this way a certain number of welds, each of them equal to about 180 mm of weld length, were performed and the tool life was measured in terms of meters of welding. The same set up was utilized

for all the three tool materials and the three process conditions, obtaining a total of nine different combinations. In Figure 8 the resulting diagrams are shown.

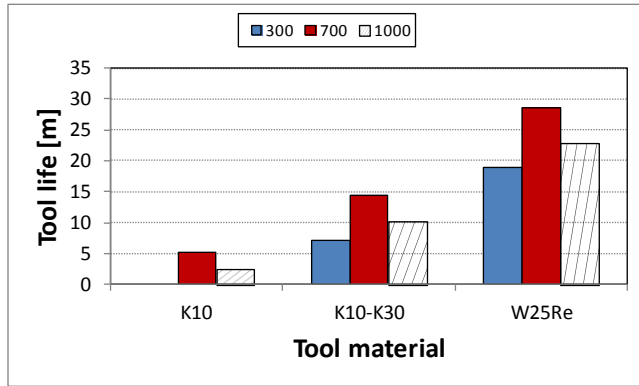


Figure 8. Tool life – total weld length to failure - at the varying of tool material and process conditions (tool rotating speed).

A few important observations can be drawn from the above figure. First, for the K10 material, no data corresponding to a rotational speed of 300 rpm is present, indicating that tool failure occurred during the first weld. It should be noticed that the test characterized by the K10 tool material and rotational speed of 300 rpm was repeated three times and always gave the same result in terms of tool early failure (the failure mode will be better discussed in the following). This is due to the combination of two factors: the brittle behavior of this alloy and the “cold” weld conditions. As a matter of fact, the lowest rotational speed corresponds to the lowest STC conferred to the joint, and, consequently, to a insufficient softening effect of the titanium sheets as related to this peculiar tool material. By increasing the STC and keeping the same tool material, a few sheets could be successfully welded. However, the overall tool life is very poor, showing the lowest values among the three materials, and resulting in unacceptable values for industrial applicability.

As far as the other two materials are regarded, a significant increase is observed in the tool life. More in details, all the values obtained at the varying of the tool rotating speed with the K10-K30 tool are larger than the maximum obtained with the K10 tool. An analogous improvement is found when comparing the W2Re tool and K10-K30 one.

The above described different behavior of the three materials corresponds to three different failure modes. Regardless of the process conditions under which they were utilized, each of the three materials showed the same morphology at the end of its service. In Figure 9 (a to c) the pictures of the three broken tools are presented.

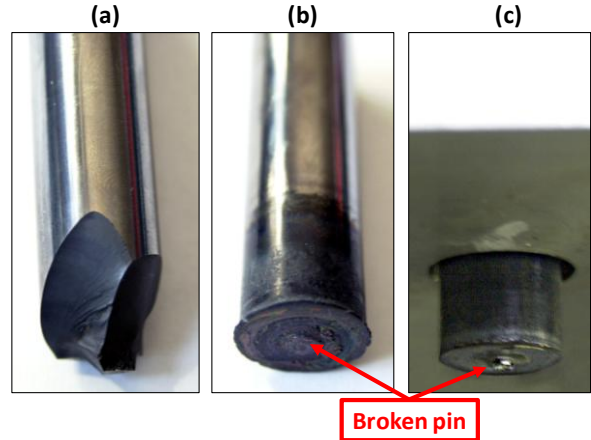


Figure 9. Broken tools at the end of their life: (a) K10, (b) K10-K30 and (c) W25Re.

As it can be seen, the two WC based alloys exhibit a completely different behavior: K10 shows a typical brittle fracture due to excess of combined torque, compressive force, and bending solicitation. Although this alloy is characterized by larger hardness with respect to the K10-K30 alloy, it also shows a reduced Transverse Rupture Strength (TRS) (see again Table 1), which can be easily connected to fracture toughness. The extreme mechanical solicitations the tool undergoes to, together with small vibrations due to random material inhomogeneities and machine not perfect stiffness, led to an early failure. This phenomenon, as already discussed, is emphasized and taken to the extreme when the “cold” process conditions are selected and no weld can be completed.

As far as the K10-K30 alloy is regarded, a ductile failure mode is observed. Severe deformation progressively occurs in the shoulder, where, at the end of the tool life, a significant mushrooming effect is found. Additionally, the final out of service of the tool is reached when the pin, previously mushroomed as well, is completely torn away from the shoulder surface. Finally, visible sign of titanium adhesive wear are found on the shoulder surface. As a consequence of the above observations, it arises that the quality of the welds progressively decreases as the tool accumulates meters of weld length.

Finally, observing the W25Re tool after failure, no evident sign of either deformation or adhesive wear is found. On the contrary, a fracture at mid height of the pin is visible, resulting in insufficient penetration in the titanium sheets and in the so called tunnel defect in the welded joints. In this way it can be stated that the tool went out of service. However, it should be observed that the broken pin does not show visible signs of deformation and mushrooming (Figure 10).

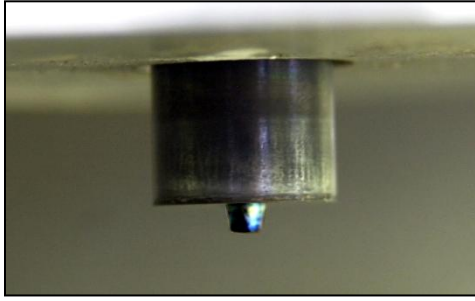


Figure 10. W25Re tool at about half of its life cycle (≈ 12 m). 700 rpm case study.

As a consequence, the quality of the welds performed with this tool is kept about constant during its service. Such consideration was substantiated by both optical analysis of the joints and mechanical testing of a few samples randomly taken during the experimental campaign.

As far as the influence of the process conditions is regarded, for all the three materials, the shortest life was found in correspondence of the lowest STC, i.e. with a tool rotation of 300 rpm. On the other hand, the maximum weld length was measured with the intermediate STC value. When the maximum STC was utilized, i.e. when the tool rotates at 1000 rpm, weld length values in between the two extremes were observed. In order to explain such behavior the numerical model was utilized to calculate both the welding forces and the temperatures reached in the tool. Thermal data of WC alloys were used for the temperature calculations. Analogous results were found for the W25Re.

Figure 11 shows the evolution of the vertical force, the main component in FSW processes, during the weld. It should be observed that the second major component, i.e. the advancing one, is usually one order of magnitude lower than the vertical force [20].

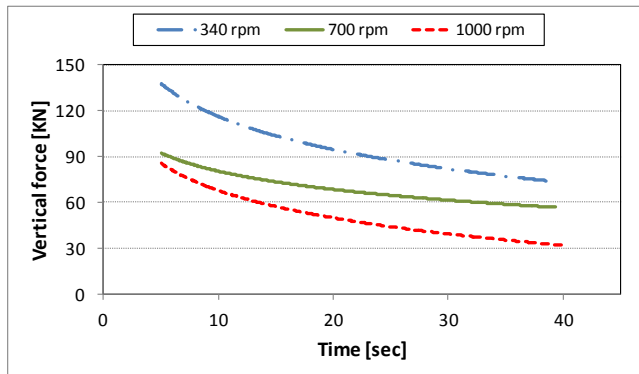


Figure 11. Calculated vertical force vs. time at the varying of the rotational speed.

The three curves show a decreasing trend till about 40 seconds, corresponding to a tool translation of about 22 mm. As previously mentioned, this is approximately the distance after which the process reaches the steady state and, from this moment on, the forces will be quite constant. As expected, the forces exerted on the tool decrease at the increasing of the tool rotation due to the increased thermal flow and, as a consequence, to the enhanced sheets material softening. However, quite large values are calculated even for the 1000 rpm case study. Additionally, it can be observed that at the beginning of the advancing stage, the magnitude of the forces is significantly larger than the one calculated for the steady state. This indicates that the final part of the sinking stage as well as the initial part of the welding stage are the process phases during which the tool experiences the most severe solicitations, ranging the vertical force between 85 kN and 140 kN. As a matter of fact, for each of the considered materials and for each of the considered process conditions, all the tools breakage occurred during these two phases.

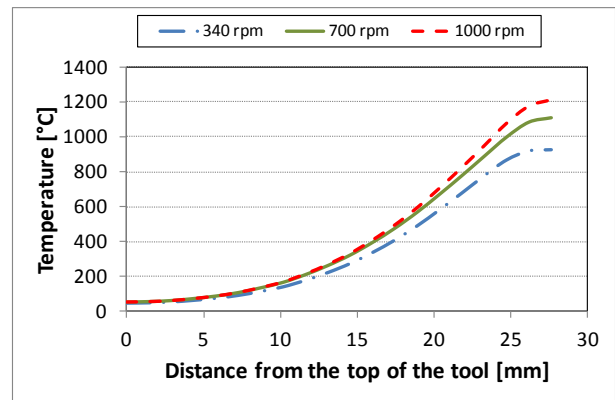


Figure 12. Calculated temperature along the tool axis at the varying of the rotational speed.

Figure 12 illustrates the temperatures profiles calculated for the tool along its axis (see again the black arrow in Figure 6). Starting from the top surface, temperature assumes similar values for the three configurations. On the contrary, getting closer to the shoulder surface and the pin, an appreciable difference is observed, reaching a maximum value of about 300° between the coldest and the hottest weld.

It is worthy notice that an increase in the tool rotation, i.e. an increase in the maximum temperature, results in an increased thermo-mechanical solicitation and may lead to a failure of the tool. On the other hand, as observed in Figure 11, at the increasing of the tool rotation the reaction force transmitted by the sheets to the tool decreases.

These two contrasting effect are summarized in Figure 13, where the maximum temperatures observed in the tool are plotted together with the steady state force value at the varying of the tool rotational speed. As anticipated, the thermal and mechanical solicitations have opposite trends at the increasing of the tool rotation. A qualitative curve, taking into account the combined effect of softening and actual load decreasing was added to the figure in order to better highlight the presence of a peculiar rotational speed value – indicated as R^* in the figure - minimizing the overall thermo-mechanical solicitation on the tool. It should be noticed that no actual minimization procedure was carried out in this research.

From the above observation it is clear why all the utilized tools showed the maximum weld length in correspondence of the intermediate STC value in spite of the significant reduction in the vertical force observed in Figure 11.

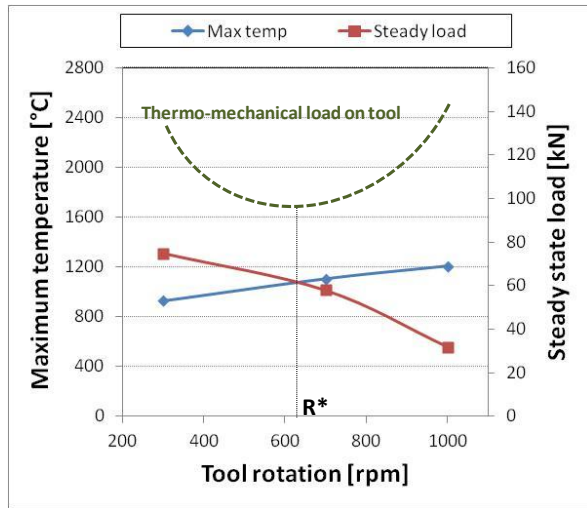


Figure 13. Maximum tool temperature and steady state vertical force vs. tool rotation; qualitative overall thermo-mechanical solicitation on the tool.

SUMMARY & CONCLUSIONS

In the paper an experimental campaign aimed to the identification of the most suited tool material for Friction Stir Welding of titanium alloys was developed. 3 mm thick Ti-6Al-4V titanium alloy sheets were welded together under three different process conditions. The same tool design was utilized for all the tests, the effectiveness of water cooling was assessed and three different ultra resistant refractory metal alloys were tested.

From the numerical and experimental obtained results the following main conclusions can be drawn:

- ✓ Water cooling on the lateral surface of refractory metal tools does not produce any significant change in the calculated tool temperature and no beneficial effect is observed for the tool life. This is due to the extremely low thermal conductivity of these materials. By adopting this tool cooling configuration, the use of a coolant chiller would not result in any appreciable improvement in the heat removal.
- ✓ All the tools failures were observed between the end of the sinking stage and the first few mm of welding. According to the numerical results, these is the process
- ✓ Although characterized by a large hardness value, the K10 material revealed as inadequate for FSW of titanium alloys as brittle fractures occur. No weld could be obtained with the low rotational speed and unsatisfying tool life values were observed at the increasing of the tool rotation;
- ✓ More encouraging results were obtained with the K10-K30 alloy, characterized by increased fracture toughness, although severe deformation was observed in the tool shoulder and pin during the tool life cycle. This aspect may seriously compromise the soundness of the obtained joints;
- ✓ The best results, both in terms of tool life and weld quality, were obtained with the W25Re tool. Satisfying tool life was obtained and no visible sign of degradation was observed during the life cycle;
- ✓ All the tools showed the largest weld length for an intermediate tool rotation value due to the concurrent effect of the force acting on the tool itself and the temperatures it experiences during the process.

After the preliminary screening of tool materials here presented, in the future the authors will focus their research activity on the W25Re alloy. Further developments include a quantitative analysis of the abrasive and adhesive wear on the W25Re tool as well as an implementation of the wear phenomenon in the numerical model.

REFERENCES

- [1] Liu, H.J., Fujii, H., Maeda, M., Nogi, K., 2003, Tensile properties and fracture locations of friction-stir-welded joints of 2017-T351 aluminum alloy, J. of Mat. Proc. Tech., 142: 692–696
- [2] Winter, E.F.M., Sharp, M.L., Nordmark, G.E., Banthia, V.K., 1990, Design considerations for aluminium spaceframe automotive structures, SAE technical series, Report No 905178.

- [3] Rhodes, C.G., Mahoney, M.W., Bingel, W.H., Spurling, R.A., Bampton, C.C., 1997, Effects of Friction Stir Welding on Microstructure of 7075 Aluminum, *Scripta Materialia*, 36: 69-75
- [4] Guerra, M., Schmidt, C., McClure, L.C., Murr, L.E., Nunes, A.C., 2003, Flow patterns during friction stir welding, *Mater Charact*, 49: 95-101
- [5] Fratini, L., Buffa, G., Shivpuri, R., 2010, Mechanical and metallurgical effects of in process cooling during friction stir welding of AA7075-T6 butt joints, *Acta Mater.*, 58: 2056
- [6] Fratini, L., Buffa, G., Micari, F., Shivpuri, R., 2009, On the material flow in FSW of T-joints: Influence of geometrical and technological parameters, *Int. J. of Adv. Manuf. Technol.*, 44: 570
- [7] Buffa, G., Campanile G., Fratini, L., Prisco, A., 2009, Friction stir welding of lap joints: Influence of process parameters on the metallurgical and mechanical properties, *Mater. Sci. and Eng. A*, 519: 19.
- [8] Gan, W., Li, Z.T., Khurana, S., 2007, Tool mushrooming in friction stir welding of L80 steel, *TMS Annual Meeting*, 279-283.
- [9] Mahoney, M., Nelson, T., Sorenson, C., Packer, S., 2010, Friction Stir Welding of Ferrous Alloys: Current Status, *Materials Science Forum*, 638-642: 41-46.
- [10] Zhang, Y., Sato, Y.S., Kokawa, H., Park, S.H.C., Hirano, S., 2008, Stir zone microstructure of commercial purity titanium friction stir welded using pcBN tool, *Materials Science and Engineering A*, 488 (1-2): 25-30.
- [11] Liu, Q., Steel, R., Peterson, J., Horman, S., Collier, M., Marshall, D.B., Davis, J.B., (...), Mahoney, M., 2010, Advances in friction stir welding tooling materials development, *Proceedings of the International Offshore and Polar Engineering Conference*, 4: 298-302.
- [12] Sato, Y.S., Miyake, M., Kokawa, H., Omori, T., Ishida, K., Imano, S., Park, S.H.C., Hirano, S., 2011, Development of a cobalt-based alloy FSW tool for high-softening-temperature materials, *2011 TMS Annual Meeting*, 3-9.
- [13] Thompson, B.T., Babu, S.S., Lolla, T., 2011, Application of diffusion models to predict FSW tool wear *Proceedings of the International Offshore and Polar Engineering Conference*, 520-526
- [14] Thompson, B., Babu, S.S., 2010, Tool degradation characterization in the friction stir welding of hard metals, *Welding Journal (Miami, Fla)*, 89 (12): 256s-261s.
- [15] Fratini, L., Micari, F., Buffa, G., Ruisi, V.F., 2010, A new fixture for FSW processes of titanium alloys, *CIRP Annals - Manufacturing Technology*, 59(1):271-274
- [16] *Hot Working Guide – A compendium processing maps (1997) ASM International.*
- [17] *Deform 3D user manual. SFTC.*
- [18] Fratini, L., Beccari, S., Buffa, G., 2005, Friction Stir Welding FEM model improvement through inverse thermal characterization, *Transactions Of The North American Manufacturing Research Institution Of SME* 33: 259-266
- [19] Buffa, G., Fratini, L., Micari, F., 2011, Mechanical and Microstructural Properties Prediction by Artificial Neural Networks in FSW Processes of Dual Phase Titanium Alloys, *Proceedings of NAMRC 39 Conference.*
- [20] Buffa, G., Hua, J., Shivpuri, R., Fratini, L., 2006, A continuum based fem model for friction stir welding - Model development, *Mat. Sci. and Eng. A*, 419/1-2: 389-396.